

# The identification of the optical companion to the binary millisecond pulsar J0610-2100 in the Galactic field

C. Pallanca<sup>1</sup>, R. P. Mignani<sup>2,3</sup>, E. Dalessandro<sup>1</sup>, F.R. Ferraro<sup>1</sup>, B. Lanzoni<sup>1</sup>, A. Possenti<sup>4</sup>,  
M. Burgay<sup>4</sup>, E. Sabbi<sup>5</sup>.

<sup>1</sup> *Dipartimento di Astronomia, Università degli Studi di Bologna, via Ranzani 1, I-40127 Bologna, Italy*

<sup>2</sup> *Mullard Space Science Laboratory, University College London, Holmbury St. Mary, Dorking, Surrey, RH5 6NT, UK*

<sup>3</sup> *Kepler Institute of Astronomy, University of Zielona Góra, Lubuska 2, 65-265, Zielona Góra, Poland*

<sup>4</sup> *INAF-Osservatorio Astronomico di Cagliari, località Poggio dei Pini, strada 54, I-09012 Capoterra, Italy*

<sup>5</sup> *Space Telescope Science Institute, 3700 San Martin Drive, Baltimore, MD 21218, USA*

June 27, 2012

## ABSTRACT

We have used deep  $V$  and  $R$  images acquired at the ESO Very Large Telescope to identify the optical companion to the binary pulsar PSR J0610–2100, one of the black-widow millisecond pulsars recently detected by the Fermi Gamma-ray Telescope in the Galactic plane. We found a faint star ( $V \sim 26.7$ ) nearly coincident ( $\delta r \sim 0''.28$ ) with the pulsar nominal position. This star is visible only in half of the available images, while it disappears in the deepest ones (those acquired under the best seeing conditions), thus indicating that it is variable. Although our observations do not sample the entire orbital period ( $P = 0.28$  d) of the pulsar, we found that the optical modulation of the variable star nicely correlates with the pulsar orbital period and describes a well defined peak ( $R \sim 25.6$ ) at  $\Phi = 0.75$ , suggesting a modulation due to the pulsar heating. We tentatively conclude that the companion to PSR J0610–2100 is a heavily ablated very low mass star ( $\approx 0.02M_{\odot}$ ) that completely filled its Roche Lobe.

*Subject headings:* Stars:Binaries:General, Stars:imaging, Stars:Pulsar:Individual: PSR J0610-2100, techniques: photometric

## 1. INTRODUCTION

It is generally accepted that millisecond pulsars (MSPs) are formed in binary systems containing a neutron star that is eventually spun up through mass accretion from an evolving companion. Among these systems those characterized by relatively small eccentricity and very small mass function (typically the companion mass is only  $M_{\text{COM}} \lesssim 0.1M_{\odot}$ ) are classified as “black-widow” pulsars (BWPs). In several cases the pulsar shows eclipses in the radio signal suggesting that the companion is a non-degenerate, possibly bloated star. In some cases the eclipse of the radio signal is so extended that it implies a size of the companion larger than its Roche lobe, suggesting that the obscuring material is plasma released by the companion because of the energy injected by the pulsar. However since the size of the eclipse depends on the inclination angle (King et al. 2005), not all BWPs are expected to show eclipses. As suggested by King et al. (2003), the formation of BWPs needs two phases: a first one in which the companion spins-up the neutron star to millisecond periods and a second where the companion is ablated by the pulsar. While it is difficult to describe the two phases using the same star as a companion to the MSP, in globular clusters (GCs), where encounters and exchange interactions are frequent, the white dwarf (WD) companion responsible for the pulsar spinning-up can be replaced by a main sequence star via an exchange interaction. The following evolution of this newly assembled binary system can cause the progressive vaporization of the companion because of the energy injected by the MSP. Since dynamical interactions are less probable in low density environments, BWPs were thought to be mainly generated in GCs and then ejected in the field. However, the increasing number of BWPs discovered in the Galactic field suggests that they must form in the disk as well. In this paper we focus on a BWP in the galactic plane: PSR J0610–2100.

PSR J0610–2100 is a MSP with period  $P = 3.8$  ms and a radio flux at 1.4 GHz of  $S_{1.4} = 0.4 \pm 0.2$  mJy discovered during the Parkes High-Latitude pulsar survey (Burgay et al. 2006, hereafter B06). The period derivative  $\dot{P} = 1.235 \times 10^{-20} \text{s s}^{-1}$  implies a characteristic age  $\tau = 5$  Gyr, a magnetic field  $B = 2.18 \times 10^8$  G, and a rotational energy loss rate  $\dot{E} = 2.3 \times 10^{33} \text{ erg s}^{-1}$ , similar to the values measured for other MSPs. PSR J0610–2100 is in a binary system, with an orbital period of  $\sim 0.28$  d. In particular, it is one of 53 binary MSPs with  $P < 10$  ms currently known in the Galactic disk (<http://www.atnf.csiro.au/research/pulsar/psrcat/expert.html>; Manchester et al. 2005). It is located at a distance of  $3.5 \pm 1.5$  kpc, estimated from its dispersion measure ( $\text{DM}=60.666 \text{ pc cm}^{-3}$ ) and the Galactic electron density model of Cordes & Lazio (2002). The pulsar has a proper motion of  $\mu_{\alpha} \cos \delta = 7 \pm 3 \text{ mas yr}^{-1}$  and  $\mu_{\delta} = 11 \pm 3 \text{ mas yr}^{-1}$  (B06), which implies a transverse velocity of  $228 \pm 53 \text{ km s}^{-1}$ , one of the highest measured for Galactic MSPs. The system mass function ( $f = 5 \times 10^{-6}$ ) implies a lower limit of  $0.02M_{\odot}$  for the mass of the companion, assuming  $1.35M_{\odot}$  for the pulsar (B06). Thus, in agreement with

the definition above, PSR J0610–2100 is probably a BWP seen at a low inclination angle (in fact no eclipse is detected).

Until a few years ago just two other BWPs were known in the Galactic field, namely PSR B1957+20 (Fruchter et al. 1988a) and PSR J2051-0827 (Stappers et al. 1996a). But very recently, thanks both to dedicated surveys of  $\gamma$ -ray sources and to new blind searches, seven new BWPs have been discovered, most of them having been detected in  $\gamma$ -rays (see Roberts 2011 and references therein). Also PSR J0610–2100 has been detected in  $\gamma$ -rays by the Large Area Telescope (LAT) on board the *Fermi* Gamma-ray Space Telescope. Based upon positional coincidence with the LAT error box, it was initially associated with the  $\gamma$ -ray source 1FGL J0610.7–2059 (Abdo et al. 2009; 2010). The detection of  $\gamma$ -ray pulsations at the radio period of PSR J0610–2100 has been recently reported and used to confirm it as the  $\gamma$ -ray counterpart to the MSP (Espinoza et al., in preparation). In the X-rays PSR J0610–2100 has not been detected, neither by the *ROSAT* All Sky Survey (Voges et al. 1999), nor by *Swift* (Marelli, private communication).

Studying the optical emission properties of binary MSP companions is important to better constrain the orbital parameters and to clarify the evolutionary status of these systems and then to track back their history and characteristic timescales. In spite of their importance, only two optical companion to BWPs in the Galactic field have been detected to date (Fruchter et al. 1988b, Reynolds et al. 2007, and Van Kerkwijk et al. 2011; Stappers et al. 1996b, Stappers et al. 1999 and Stappers et al. 2000). The binary MSP PSR B1957+20 is the first discovered BWP and one of the best studied members of this class. The optical companion to PSR B1957+20 was identified by Kulkarni et al. (1988), while subsequent observations found the companion to vary by a fraction of 30%-40% in flux over the course of the orbital period (Callanan et al. 1995). Reynolds et al. (2007), modelling the light curve over all the orbital period, constrained the system inclination  $63^\circ < i < 67^\circ$  and the filling factor of the Roche Lobe ( $0.81 < f < 0.87$ ). Moreover, they ruled out the possibility that the companion is a white dwarf, suggesting that most probably is a brown dwarf. A recent spectroscopic analysis, combined with the knowledge of the inclination angle inferred from models of the light curve, suggested that the PSR B1957+20 is massive with  $M_{\text{PSR}} = 2.4M_\odot$  ( $M_{\text{PSR}} > 1.66M_\odot$  being conservative; van Kerkwijk et al. 2011). The optical companion to binary PSR J2051-0827 was identified by Stappers et al. (1996b). They found that the amplitude of the companion’s light curve was at least 1.2 mag, and that the variation was consistent with the companion’s rotating synchronously about the pulsar and one side being heated by the impinging pulsar flux. In subsequent works it has been possible to study the entire lightcurve, measuring amplitudes of 3.3 and 1.9 magnitudes in the *R*-band and *I*-band respectively. The companion star has been modelled by a gravitationally distorted low-mass secondary star which is irradiated by the impinging pulsar wind. The resulting

best-fit model is of a Roche lobe filling companion star which converts approximately 30% of the incident pulsar spin down energy into optical flux (Stappers et al., 2000).

Here we present the first identification of the optical companion to PSR J0610–2100, from data acquired at the ESO *Very Large Telescope* (VLT). The observations and data analysis are described in Sect. 2, while the results are presented in Sect. 3 and discussed in Sect. 4.

## 2. OBSERVATIONS AND DATA ANALYSIS

The photometric data set used for this work consists of a series of ground-based optical images acquired with the FOcal Reducer/low dispersion Spectrograph 2 (FORs2) mounted at the ESO-VLT. We used the Standard Resolution Collimator, with a pixel scale of  $0.25''/\text{pixel}$  and a field of view (FOV) of  $6.8' \times 6.8'$ . In order to obtain deep images free from the blooming due to heavy saturation of bright stars, which can significantly limit the search for faint objects, all the brightest stars in the FOV have been covered with occulting masks.

Six short acquisition images (of 5 s each) and a total of 29 deep images in the  $V_{\text{BESSEL}}$  and  $R_{\text{SPECIAL}}$  bands ( $V$  and  $R$  hereafter) were collected during six nights, from mid December 2004 to the beginning of January 2005 (see Table 1), under program 074.D – 0371(A) (PI: E. Sabbi). These data allow us to sample  $\sim 25\%$  of the orbital period in  $V$  and less than 40% of it in  $R$  (see column 4 in Table 1).

By following standard reduction procedures, we corrected the raw images for bias and flat-field. In particular, in order to obtain high-quality master-bias and master-flat images, we selected a large number of images obtained during each observing night and, for each filter, we properly combined them by using the tasks `zerocombine` and `flatcombine` in the IRAF package `CCDRED`. The calibration files thus obtained have been applied to the raw images by using the dedicated task `ccdproc`.

Based on the World Coordinate System (WCS) of the images, we approximately located the pulsar position and decided to limit the photometric analysis to a region of  $500 \text{ pixel} \times 500 \text{ pixel}$  ( $\sim 125'' \times 125''$ ) centered on it.

We carried out the photometric analysis by using `DAOPHOT` (Stetson 1987, 1994). We modeled the point spread function (PSF) in each image by using about forty bright, isolated and not saturated stars. The PSF model and its parameters have been chosen by using the `DAOPHOT` PSF routine on the basis of a Chi-square test, with a Moffat function (Moffat 1969) providing the best fit to the data in all cases.

Since our purpose is to detect the faintest stars in the field, we selected the three images obtained under the best seeing conditions ( $\sim 0.6''$ ) in both filters and we combined them using the IRAF task `imcombine` in order to obtain a high signal to noise (S/N) master frame to be used as a reference for the object detection. This was done by using the DAOPHOT FIND routine and imposing a detection limit of  $3\sigma$ .

Finally, by using `allframe` (Stetson 1987, 1994) we forced the object detection and PSF fitting in each single image adopting the star positions in the master frame as reference. This procedure also allowed us to achieve an improved determination of the star centroids and a better reconstruction of the star intensity profiles.

*Photometric calibration:* For a straightforward comparison with theoretical models able to provide information about luminosity and temperature of the companion star, we decided to calibrate the instrumental magnitudes to the standard Johnson photometric system. To this aim, we first derived the calibration equation for ten standard stars in the field PG0231 (Stetson 2000), which has been observed with FORS2 during a photometric night (December 17, 2004) in both  $V$  and  $R$  under a calibration program. To analyze the standard star field we used the DAOPHOT PHOT task and performed aperture photometry with a radius  $r = 14$  pixels beyond which the contribution of the PSF wings to the star intensity profile becomes negligible. We then compared the obtained magnitudes with the standard Stetson catalog available on the CADC web site<sup>1</sup>. The resulting calibration equations are  $V = v - 0.092(v - r) + 27.79$  and  $R = r - 0.019(v - r) + 27.97$ , where  $v$  and  $r$  are the instrumental magnitudes. The color coefficient is very small for the  $R$  band, while it could be not negligible in the  $V$  band.

*Astrometry:* Since the pulsar timing position is known with a very high precision, obtaining accurate astrometry is a critical requirement in searching for the optical companions to binary MSPs. For this reason, particular care has been devoted to obtain a very good astrometric solution. Since most of the astrometric standard stars are saturated in our catalog, we used the short  $R$ -band to this purpose. As a first step of our procedure, we registered the pixel coordinates of this image onto the absolute coordinate system through the cross-correlation of about one hundred primary astrometric standards from Guide Star Catalog II (GSCII - STScI, 2001; Lasker et al. 2008), by using CataXcorr<sup>2</sup>. We then used about fifty not saturated stars in common between the reference and our general catalogs as secondary astrometric standards. At the end of the procedure the typical accuracy of the astrometric

---

<sup>1</sup><http://cadewww.dao.nrc.ca/community/STETSON/standards/>

<sup>2</sup>CataXcorr is a code aimed at cross-correlating catalogues and finding astrometric solutions, developed by P. Montegriffo at INAF - Osservatorio Astronomico di Bologna. This package has been used in a large number of papers of our group in the past 10 years.

solution was  $\sim 0''.2$  in both right ascension ( $\alpha$ ) and declination ( $\delta$ ).

### 3. THE COMPANION TO PSR J0610-2100

In order to identify the companion to PSR J0610–2100 we first searched for objects with coordinates compatible with the nominal PSR position:  $\alpha = 06^h10^m13^s.59214(10)$ ,  $\delta = -21^\circ00'28''.0158(17)$  at Epoch MJD=53100 (B06). Since the epoch of observations is within less than one year from the epoch of the reference radio position, we neglected the effect of proper motion, which is much smaller than the accuracy of the astrometric solution of the FORS2 images.

A first visual inspection of the pulsar region clearly shows that only one star lies within a couple of arcseconds from the MSP radio position: it is located at  $\alpha = 06^h10^m13^s.58$   $\delta = -21^\circ00'27''.83$ , just  $0''.28$  from PSR J0610–2100. Thus, from positional coincidence alone, we found a very good candidate companion to PSR J0610–2100. Note that the chance coincidence probability<sup>3</sup> that a star is located at the pulsar position is only  $P = 0.0007$ . Hence, this star is the companion to PSR J0610–2100 with a probability of  $\sim 99\%$ . Interestingly enough, this star was not present in the master object list obtained from the stacking of the  $R$ -band images because it is visible in only half of the images, while it completely disappears in the others (see Figure 1). We performed a detailed photometric analysis of this star for measuring its magnitude in as many images as possible, and we found that it is not detected in the deepest  $R$  images obtained under the best seeing conditions ( $FWHM \sim 0.6''$ ). In summary, we were able to measure the magnitude of the star in only 12 images (10 in the  $R$ -band and 2 in the  $V$ -band), finding significant variations:  $\delta R \sim 1$  mag, from  $R = 25.3 \pm 0.1$  to  $R = 26.3 \pm 0.2$ , and  $\delta V \sim 0.5$  mag, from  $V = 26.7 \pm 0.2$  to  $V = 27.2 \pm 0.2$ . In the remaining images the star magnitude is below the detection threshold ( $R = 27 \pm 0.3$  and  $V = 27.3 \pm 0.3$ ), thus suggesting a much more pronounced optical variation. Considering the entire data set, the object’s photometry shows a quite large scatter, significantly ( $> 5\sigma$ ) larger than that computed for stars of similar magnitude in the same FOV (see Figure 2). These findings confirm that this is a variable object near the detection limit of our sample.

In order to establish a firm connection between this star and the pulsar we computed the  $V$  and  $R$  light curves folding each measurement with the orbital period ( $P = 0.2860160010$  d) and the ascending node ( $T_0 = 52814.249433$ ) from the radio ephemeris (B06). As shown

---

<sup>3</sup>The chance coincidence probability is calculated as  $P = 1 - \exp(-\pi\sigma R^2)$  where  $\sigma$  is the stellar density of stars with similar magnitude to the candidate companion and  $R$  is the accuracy of the astrometric solution.

in Figure 3, although the available data do not allow a complete coverage of the orbital period, the flux modulation of the star nicely correlates with the pulsar orbital phase. The available data are consistent with the rising (in the  $V$  band) and the decreasing (in  $R$ -band) branches of a light curve with a peak at  $\Phi = 0.75$ . This is the typical behaviour expected when the surface of the companion is heated by the pulsar flux and the orbital plane has a sufficiently high inclination angle. In fact, in this configuration a light curve with a maximum at  $\Phi = 0.75$  (corresponding to the pulsar inferior conjunction, when the companion surface faces the observer) and a minimum at  $\Phi = 0.25$  (corresponding to the pulsar superior conjunction) is expected. Indeed the star is not detectable at the epochs corresponding to the orbital phases where the luminosity minimum is predicted.

Based on all these pieces of evidence we propose the identified variable star as the companion to the pulsar; according to previous papers (see Ferraro et al. 2001, 2003; Cocozza et al 2006 and Pallanca et al. 2010), we name it COM J0610–2100.

Since the available  $V$  and  $R$  measurements are mainly clustered toward the maximum of the emission, but do not allow to precisely determine it, we used a simple sinusoidal function<sup>4</sup> to obtain a first-guess modeling of the light curve. In the following analysis we will use these values instead of the mean magnitudes over the entire orbital period. In fact, while the latter would be more appropriate in general, they are not available in this case because of the incomplete sampling of the period. Also note that during the calibration procedure the color term entering the equations has been computed as the difference between the average value of the available  $V$  and  $R$  instrumental magnitudes. While this is strictly correct for non variable stars, in the case of COM J0610–2100 it could have introduced an error in the estimated magnitudes. Since in the calibrating equations the coefficients of the color terms are very small, especially in the  $R$ -band, this uncertainty should be negligible. The resulting magnitudes of COM J0610–2100 at maximum are  $R = 25.6$  and  $V = 26.7$ . Figure 4 shows the position in the  $(R, V - R)$  color-magnitude diagram (CMD) of COM J0610–2100 and the stars detected within  $30''$  from it. For the sake of clarity a simulation of the Galactic disk population in the direction of PSR J0610–2100 computed with the Besancon Galaxy model (Robin et al. 2003) is also shown. As can be seen, COM J0610–2100 is located at a slightly bluer color with respect to the reference main sequence, thus suggesting that it probably is a non degenerate, low mass, swollen star. Indeed similar objects have been previously identified in Galactic globular clusters (see Ferraro et al. 2001, Edmonds et al 2002, Cocozza et al. 2006 and Pallanca et al. 2010).

---

<sup>4</sup> Although this assumption is not supported by a physical reason, it provides a first estimate of the magnitude and colour of COM J0610-2100 at maximum.

#### 4. DISCUSSION

We have determined the physical parameters of COM J0610–2100 from the comparison of its position in the CMD (Figure 4) with a reference zero age main sequence, assuming an interstellar extinction of  $E(B - V) \sim 0.074^5$  and the typical metallicity of the Galactic disk ( $Z = 0.02$ ). The resulting effective temperature and bolometric luminosity of the star are  $T_{eff} \sim 3500$  K and  $L_{bol} \sim 0.0017L_{\odot}$  respectively, with a conservative uncertainty of  $\pm 500$  K and  $\pm 0.0001L_{\odot}$ . Under the assumption that the optical emission of COM J0610–2100 is well reproduced by a blackbody (BB), it is possible to derive its radius:  $R_{BB} \sim 0.14R_{\odot}$ . However, since the companion to a BWP is expected to be affected by the tidal distortion exerted by the pulsar and to have filled its Roche Lobe, the dimension of the Roche Lobe might be a more appropriate value (i.e., see PSR J2051-0827; Stappers et al. 1996b and Stappers et al. 2000). According to Eggleton (1983) we assume:

$$R_{RL} \simeq \frac{0.49q^{\frac{2}{3}}}{0.6q^{\frac{2}{3}} + \ln\left(1 + q^{\frac{1}{3}}\right)}$$

where  $q$  is the ratio between the companion and the pulsar masses ( $M_{COM}$  and  $M_{PSR}$ , respectively). This relation can be combined with the PSR mass function  $f(i, M_{PSR}, M_{COM}) = (M_{COM} \sin i)^3 / (M_{COM} + M_{PSR})^2$  by assuming a NS mass  $M_{PSR} = 1.5M_{\odot}$  (as recently estimated for recycled pulsars by Ozel et al. 2012; see also Zhang et al. 2011 and Kiziltan et al. 2011), thus yielding  $R_{RL}(i) \sim 0.24 - 0.47R_{\odot}$ , depending on the inclination angle ( $i$ ) of the orbital system. These values are about 1.7-3.4 times larger than  $R_{BB}$ . In the following discussion we assume the value of the Roche Lobe as a measure of the size of COM J0610–2100 and we discuss how the scenario would change by using  $R_{BB}$  instead of  $R_{RL}$ . While these assumptions trace two extreme possibilities, the situation is probably in the midway. In fact, in the case of a completely filled Roche Lobe, the mass lost from the companion should produce some detectable signal in the radio band (unless for very small orbital inclinations) and ellipsoidal variations could be revealed in the light curve (unless the heating from the pulsar is dominating).

Under the assumption that the optical variation shown in Figure 3 is mainly due to irradiation from the MSP reprocessed by the surface of COM J0610–2100 we can estimate how the re-processing efficiency depends on the inclination angle and, hence, on the companion mass. To this end, we compare the observed flux variation ( $\Delta F_{obs}$ ) between the maximum ( $\Phi = 0.75$ ) and the minimum ( $\Phi = 0.25$ ) of the light curve, with the expected flux variation

---

<sup>5</sup> from NED, Nasa/ipac Extragalactic Database - Galactic Extinction Calculator available at the web site <http://ned.ipac.caltech.edu/forms/calculator.html>.



( $\Delta F_{exp}$ ) computed from the rotational energy loss rate ( $\dot{E}$ ). Actually, since we do not observe the entire light curve,  $\Delta F_{obs}$  can just put a lower limit to the reprocessing efficiency. Moreover, since these quantities depend on the inclination angle of the system (see below) we can just estimate the reprocessing efficiency as function of  $i$ .

At first we have to convert the observed magnitude variation into a flux. We limited our analysis to the  $R$  band since we have more observations and a more reliable sampling of the light curve. At maximum ( $\Phi = 0.75$ ) we assume  $R = 25.6$ , and between  $\Phi = 0.75$  and  $\Phi = 0.25$  we estimate an amplitude variation  $\Delta R \gtrsim 1.5$ . Hence we obtaine  $\Delta F_{obs} \sim 1.88 \times 10^{-30} \text{ erg s}^{-1} \text{ cm}^{-2} \text{ Hz}^{-1}$  and considering the filter width ( $\Delta\lambda = 165 \text{ nm}$ ) we have  $\Delta F_{obs} \sim 3.4 \times 10^{-15} \text{ erg s}^{-1} \text{ cm}^{-2}$ .

On the other hand, the expected flux variation between  $\Phi = 0.75$  and  $\Phi = 0.25$  is given by

$$\Delta F_{exp}(i) = \eta \frac{\dot{E}}{A^2} R_{\text{COM}}^2 \frac{1}{4\pi d_{\text{PSR}}^2} \varepsilon(i)$$

where  $\eta$  is the re-processing efficiency under the assumption of isotropic emission,  $A$  is semi-major axis of orbit which depends on the inclination angle,  $R_{\text{COM}}$  is the radius of the companion star, which we assumed to be equal to  $R_{\text{RL}}(i)$ ,  $d_{\text{PSR}}$  is the distance of pulsar (3.5 kpc <sup>6</sup>) and  $\varepsilon(i)$  is the fraction of the re-emitting surface visible to the observer<sup>7</sup>. By assuming  $\Delta F_{obs} = \Delta F_{exp}(i)$  between  $\Phi = 0.75$  and  $\Phi = 0.25$ , we can derive a relation linking the re-processing efficiency and the inclination angle. The result is shown in Figure 5. The absence of eclipses in the radio signal allows us to exclude very high inclination angles. As shown in Figure 5, pulsar companions with stellar mass above the physical limit for core hydrogen burning star (i.e., with  $M \geq 0.08M_{\odot}$ ) necessarily imply a non-isotropic emission mechanism of the pulsar flux (otherwise a larger than 100% physical efficiency would be required). On the contrary a re-processing efficiency between 40% and 100% is sufficient for less massive companions and intermediate inclination angles.

Taking into account the uncertainty on the pulsar distance, only re-processing efficiencies larger than  $\sim 60\%$  for inclination angles in excess to  $50^\circ$  and companion masses lower than  $\sim 0.03M_{\odot}$  are allowed in the case of the distance upper limit (5 kpc). Instead, in case of a closer distance  $\eta$  decreases for all inclination angles, thus making acceptable also companion

---

<sup>6</sup>In these calculations we adopted a distance of 3.5 kpc, while we discuss below how the scenario changes by varying the distance between the range of values within the quoted uncertainty.

<sup>7</sup> In the following we assume  $\varepsilon(i) = i/180$ . In fact, for a face-on configuration ( $i = 0^\circ$ ) no flux variations are expected, while for an edge-on system ( $i = 90^\circ$ ) the fraction of the heated surface that is visible to the observer varies between 0.5 (for  $\Phi = 0.75$ ) to zero (for  $\Phi = 0.25$ ).

stars with masses larger than  $0.08M_{\odot}$ . For instance, for companions masses between  $0.08$  and  $0.2M_{\odot}$  and a 2 kpc distant pulsar, the re-processing efficiency ranges between 30% and 60% for any value of  $i$ .

The observed optical modulation can be reproduced considering a system seen at an inclination angle of about  $60^{\circ}$ , with a very low mass companion ( $M_{\text{COM}} \sim 0.02M_{\odot}$ ) that has filled its Roche Lobe, and a re-processing efficiency of about 50%. On the other hand, if we use  $R_{\text{BB}}$  instead of the  $R_{\text{RL}}$ , the efficiency becomes larger than 100% for every inclination angle, and the only possible scenario would be that of an anisotropic pulsar emission. However, even with this assumption it is very difficult to obtain an acceptable value for  $\eta$ . This seems to confirm that  $R_{\text{BB}}$  is too small to provide a good estimate of the star physical size. Forthcoming studies will allow us to better constrain the system parameters.

## 5. ACKNOWLEDGEMENT

We thank the Referee Scott Ransom for the careful reading of the manuscript and the useful comments. This research is part of the project COSMIC-LAB funded by the European Research Council (under contract ERC-2010-AdG-267675). We thank G. Cocozza for useful discussions.

## REFERENCES

- Abdo, A. A., Ackermann, M., Ajello, M., et al. 2009, *Science*, 325, 848
- Abdo, A. A., Ackermann, M., Ajello, M., et al. 2010, *ApJS*, 188, 405
- Burgay, M., Joshi, B. C., D’Amico, N., et al. 2006, *MNRAS*, 368, 283
- Callanan, P. J., van Paradijs, J., & Rengelink, R. 1995, *ApJ*, 439, 928
- Cocozza, G., Ferraro, F. R., Possenti, A., & D’Amico, N. 2006, *ApJ*, 641, L129
- Cordes, J. M., & Lazio, T. J. W. 2002, arXiv:astro-ph/0207156
- Edmonds, P. D., Gilliland, R. L., Camilo, F., Heinke, C. O., & Grindlay, J. E. 2002, *ApJ*, 579, 741
- Eggleton, P. P. 1983, *ApJ*, 268, 368
- Ferraro, F. R., Possenti, A., D’Amico, N., & Sabbi, E. 2001, *ApJ*, 561, L93

- Ferraro, F. R., Possenti, A., Sabbi, E., & D’Amico, N. 2003, *ApJ*, 596, L211
- Fruchter, A. S., Stinebring, D. R., & Taylor, J. H. 1988a, *Nature*, 333, 237
- Fruchter, A. S., Gunn, J. E., Lauer, T. R., & Dressler, A. 1988b, *Nature*, 334, 686
- King, A. R., Davies, M. B., & Beer, M. E. 2003, *MNRAS*, 345, 678
- King, A. R., & Beer, M. E. 2005, *Binary Radio Pulsars*, 328, 429
- Kızıltan, B. 2011, in “Astrophysics of neutro stars 2010: A conference in honor of M. Ali Alpar” , AIP Conference Proceedings, Vol. 1379, pp. 41-47
- Kulkarni, S. R., Djorgovski, S., & Fruchter, A. S. 1988, *Nature*, 334, 504
- Lasker, B. M., Lattanzi, M. G., McLean, B. J., et al. 2008, *AJ*, 136, 735
- Manchester, R. N., Hobbs, G. B., Teoh, A., & Hobbs, M. 2005, *VizieR Online Data Catalog*, 7245, 0
- Moffat, A. F. J. 1969, *A&A*, 3, 455
- Ozel, F., Psaltis, D., Narayan, R., & Santos Villarreal, A. 2012, *ApJ* submitted, arXiv:1201.1006
- Pallanca, C., Dalessandro, E., Ferraro, F. R., et al. 2010, *ApJ*, 725, 1165
- Reynolds, M. T., Callanan, P. J., Fruchter, A. S., et al. 2007, *MNRAS*, 379, 1117
- Roberts, M. S. E. 2011, *American Institute of Physics Conference Series*, 1357, 127
- Robin, A. C., Reylé, C., Derrière, S., & Picaud, S. 2003, *A&A*, 409, 523
- Stappers, B. W., Bailes, M., Lyne, A. G., et al. 1996a, *ApJ*, 465, L119
- Stappers, B. W., Bessell, M. S., & Bailes, M. 1996b, *ApJ*, 473, L119
- Stappers, B. W., van Kerkwijk, M. H., Lane, B., & Kulkarni, S. R. 1999, *ApJ*, 510, L45
- Stappers, B. W., van Kerkwijk, M., & Bell, J. F. 2000, *IAU Colloq. 177: Pulsar Astronomy - 2000 and Beyond*, 202, 627
- Stetson, P. B. 1987, *PASP*, 99, 191
- Stetson, P. B. 1994, *PASP*, 106, 250

Stetson, P. B. 2000, *PASP*, 112, 925

van Kerkwijk, M. H., Breton, R. P., & Kulkarni, S. R. 2011, *ApJ*, 728, 95

Voges, W., Aschenbach, B., Boller, T., et al. 1999, *A&A*, 349, 389

Zhang, C. M., Wang, J., Zhao, Y. H., et al. 2011, *A&A*, 527, A83

FILTER	$N \times t_{exp}$	Night	PSR-Phase	Detection
$V_{BESSEL}$	$6 \times 1010$ s	17/12/04	0.04-0.26	NO
$V_{BESSEL}$	$3 \times 1010$ s	20/12/04	0.58-0.67	YES <sup>1</sup>
$R_{SPECIAL}$	$5 \times 590$ s	14/12/04	0.73-0.83	YES
$R_{SPECIAL}$	$5 \times 590$ s	21/12/04	0.06-0.16	NO
$R_{SPECIAL}$	$5 \times 590$ s	05/01/05	0.26-0.36	NO
$R_{SPECIAL}$	$5 \times 590$ s	06/01/05	0.76-0.86	YES

Table 1: <sup>1</sup> Detected in only 2 images out of 3

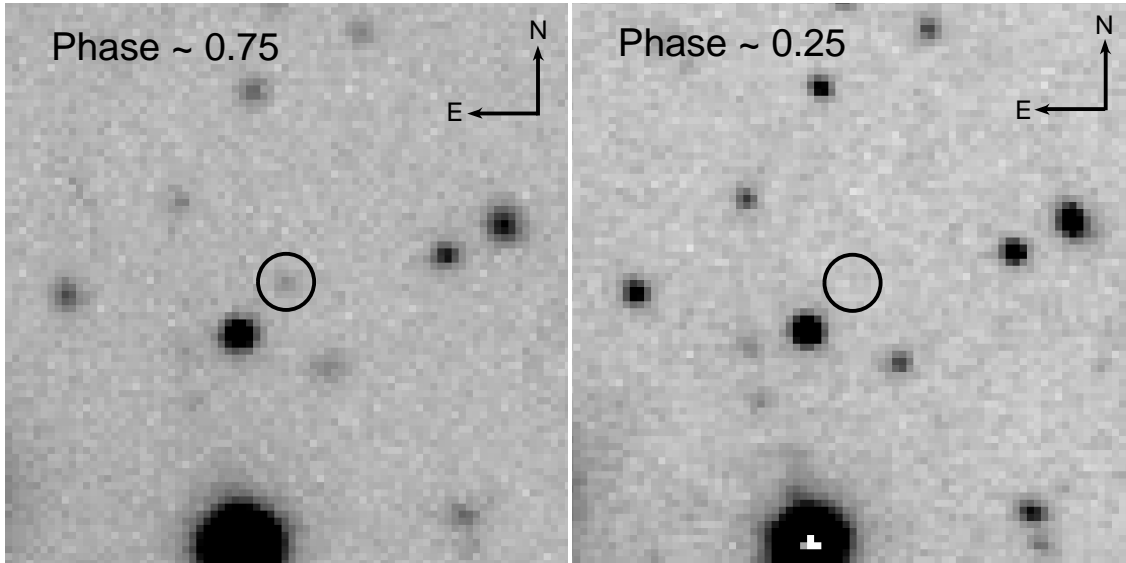


Fig. 1.—  $R$ -band images of the  $20'' \times 20''$  region around the nominal position of PSR J0610–2100, at two different epochs corresponding to the orbital phases  $\Phi = 0.75$  (left panel) and  $\Phi = 0.25$  (right panel). Each image is the average of 3 images. The circle of radius  $1''$  marks the pulsar position. A star is clearly visible in the left panel, while it vanishes in the right panel. Note that the images at  $\Phi = 0.25$  (where the star is undetected) have been obtained under the best seeing conditions ( $FWHM = 0.6''$ ).

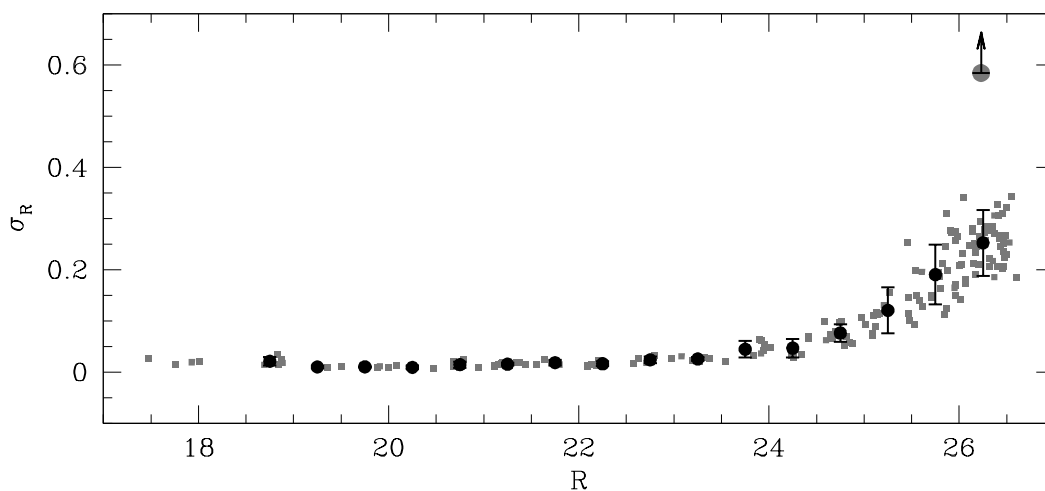


Fig. 2.— Frame to frame scatter (gray points) for the 173 stars identified in a  $125'' \times 125''$  region around the nominal PSR position, as a function of the  $R$  magnitude. The standard deviation  $\sigma_R$  has been computed by using all the available images. Black circles and the corresponding error bars are the mean and the standard deviation values in 0.5 magnitude bins, respectively. The mean magnitude ( $R \sim 26.2$ ) and standard deviation ( $\sigma_R \sim 0.6$ ) of the companion star to PSR J0610-2100 (large grey circle) likely represent lower limits to the true values, because they have been computed adopting  $R = 27$  (the  $R$ -band detection limit) in all images where the star was not visible.

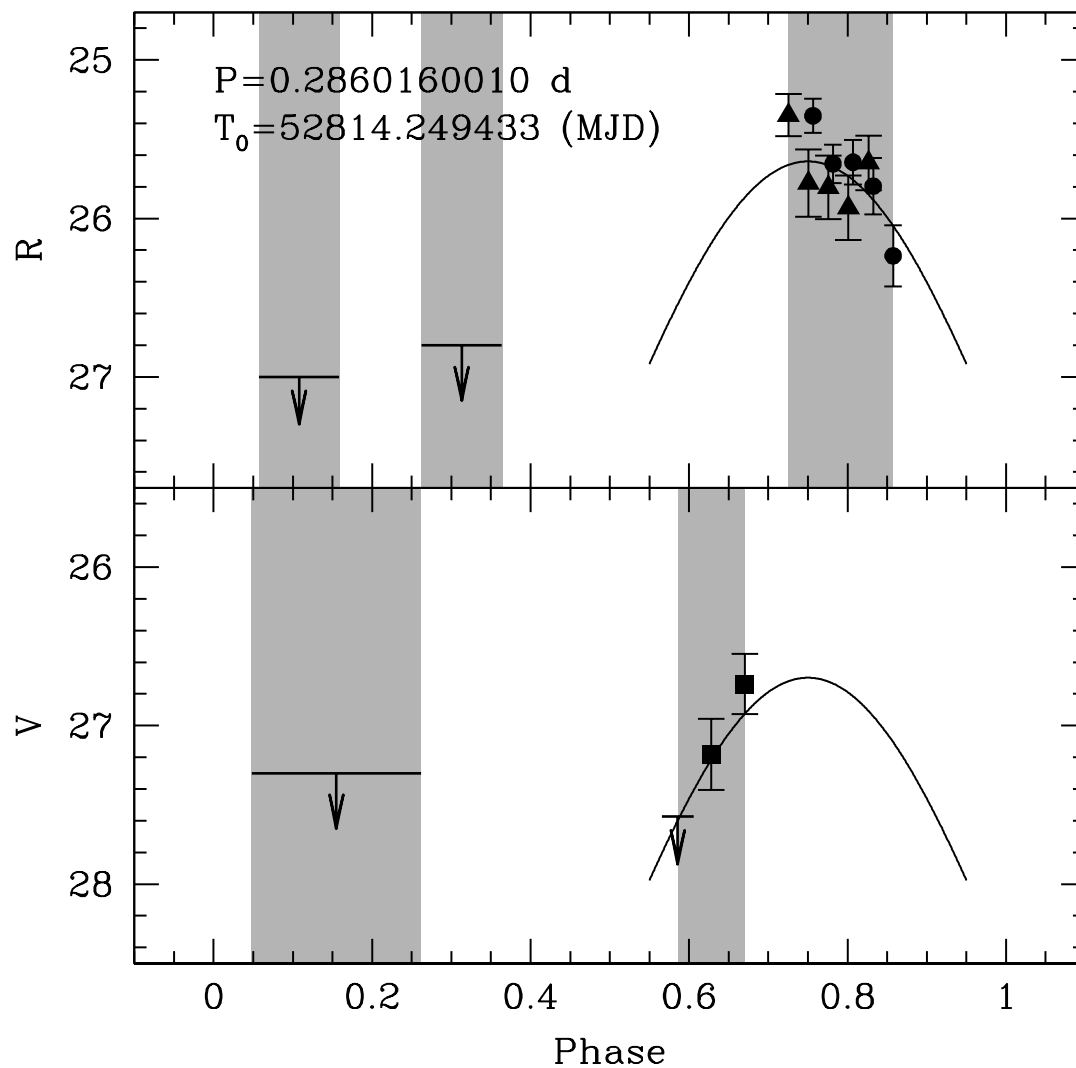


Fig. 3.— The observed light curve of the companion to PSR J0610–2100 folded with the orbital period ( $P$ ) of the pulsar using the reference epoch ( $T_0$ ) known from radio observations (B06). The different symbols represent images obtained in different nights. The horizontal lines with arrows are the estimated magnitude upper-limits for the images where the star is below the detection threshold. The gray regions correspond to the fraction of the orbital phase sampled by each observations. The solid black line is a first-guess modeling of the light curve by means of a simple mode.

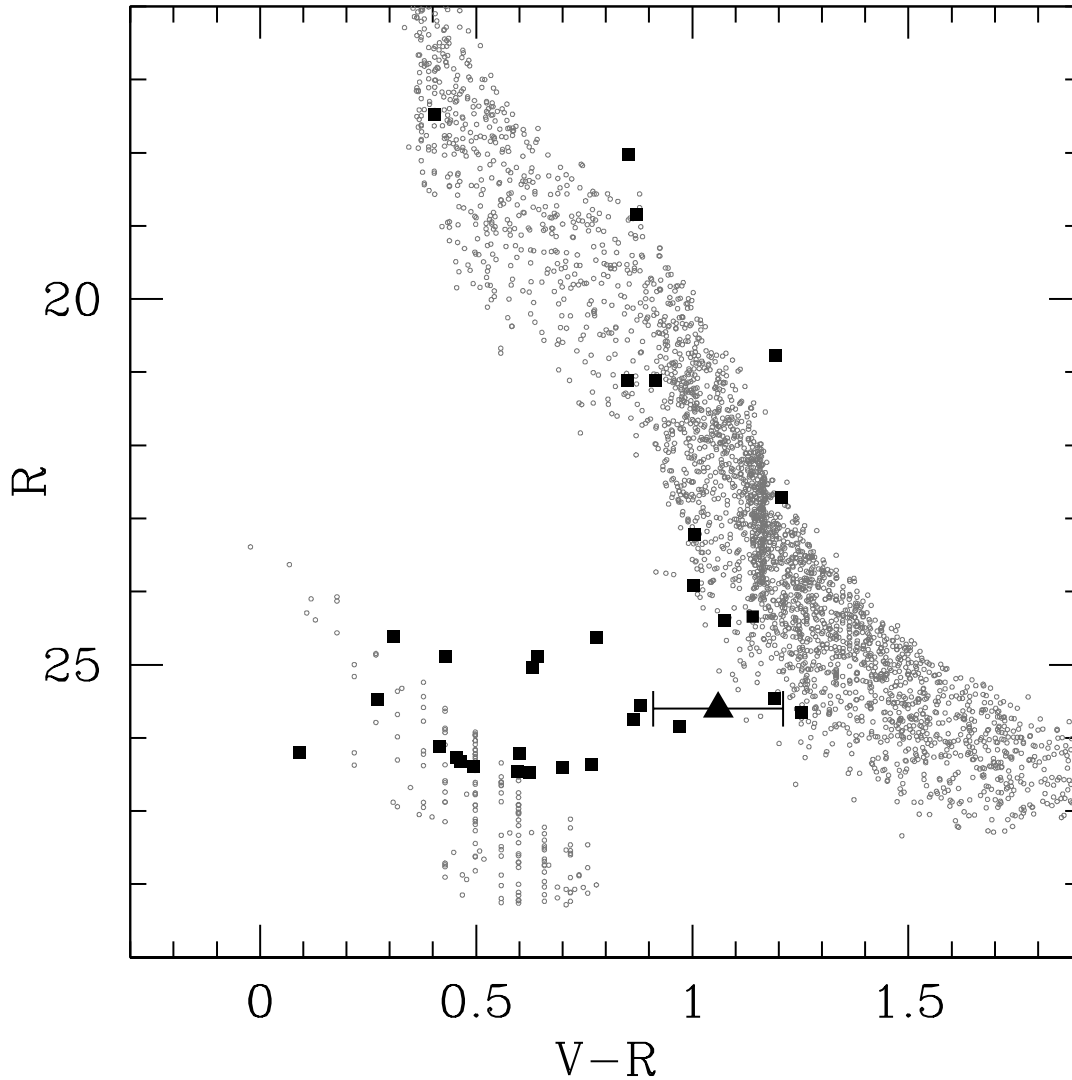


Fig. 4.—  $(R, V - R)$  color-magnitude diagram for COM J0610–2100 (large black triangle) and for the objects detected in a circle of about  $30''$  around its nominal position (black squares). COM J0610–2100 is located at  $V = 26.7$  and  $R = 25.6$ , corresponding to the values estimated from the first-guess light-curve at its maximum ( $\Phi = 0.75$ ). The error bar corresponds to the photometric error at those magnitude values. The open gray circles represent the Galaxy disk population obtained with the Besancon model (Robin et al. 2003) in the direction of the pulsar and for a distance between 2 and 6 kpc.



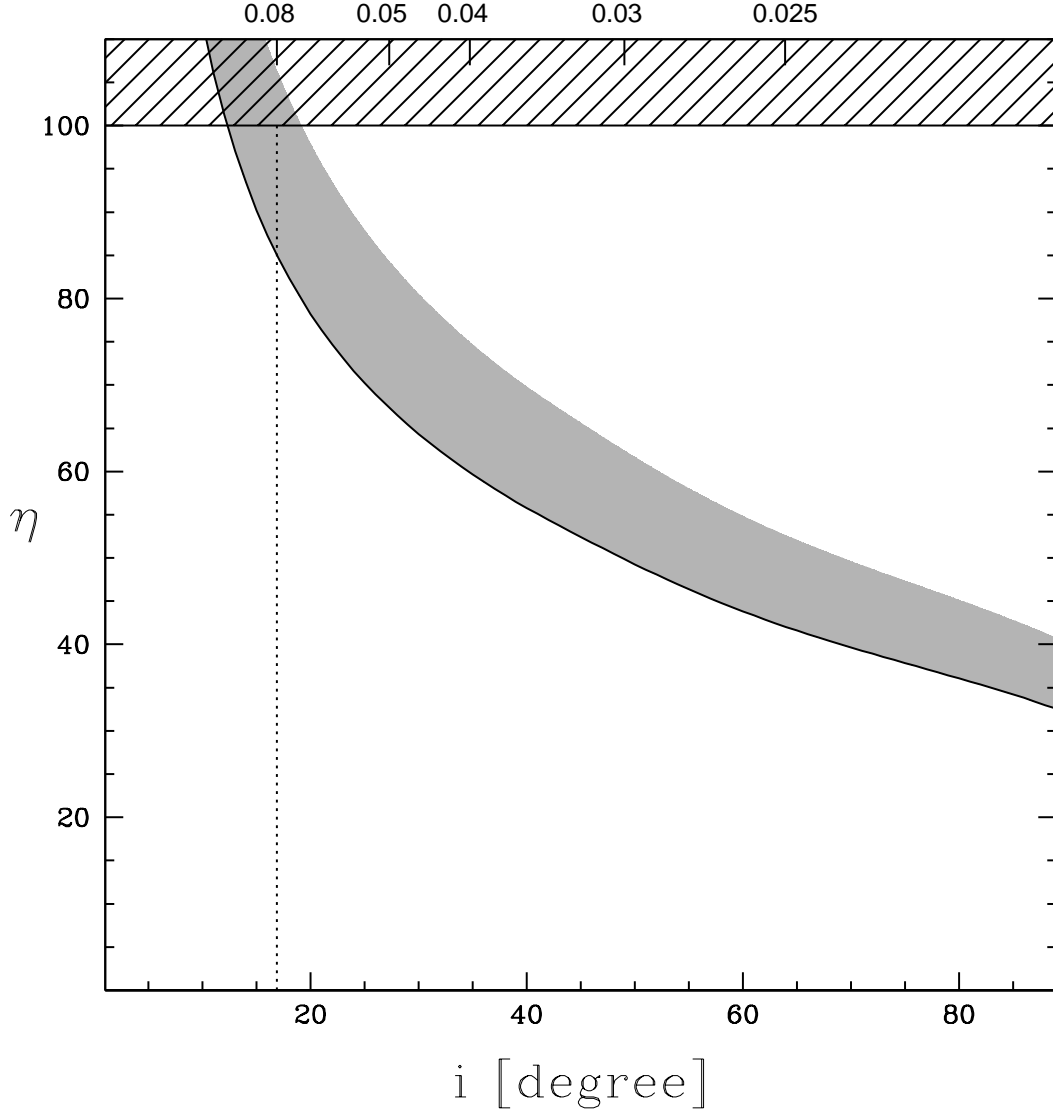


Fig. 5.— The reprocessing efficiency for isotropic emission ( $\eta$ ) as a function of the inclination angle ( $i$ ) calculated assuming  $M_{\text{PSR}} = 1.5M_{\odot}$  and  $R_{\text{COM}} = R_{\text{RL}}(i)$ . The corresponding values for the companion mass in units of  $M_{\odot}$  are reported on the top axis. The solid line corresponds to the lower limit of the amplitude of variation ( $\Delta R = 1.5$ ), while the gray region to values of  $\Delta R$  up to 3, that should be appropriate if considering the entire light curve (i.e., see PSR J2051-0827; Stappers et al. 1996b). The shaded area marks the region of the diagram where only anisotropic emission of the re-processed flux is admitted (in case of isotropy, in fact, the efficiency would be unphysical:  $\eta > 100\%$ ). The dotted line marks the physical limit for core hydrogen burning stars (i.e., objects with masses  $\geq 0.08M_{\odot}$ ).